Stress - Strain Distribution near Crack Tips and Fracture Mechanisms in Fatigue of Metals

by Shuji Taira and Keisuke Tanaka
Dept. of Mechanical Engng., Kyoto University, Kyoto, Japan

The distributions of stress and strain in the vicinity of fatigue crack tips were measured by means of the X-ray microbeam back-reflection Debye method and optical microscopy, and were compared with the results of theoretical analyses based on Dugdale's and Rice's models. The rate of fatigue crack growth was discussed by combining the data of microscopic observations with fracture mechanisms.

The materials employed in this study were five carbon steels with the carbon content ranging from 0.001 to 0.31%. The specimens were fatigued under completely reversed cyclic loads at room temperature in fatigue testing machines operated with a frequency of 2,000 cpm.

Stress-Strain Distribution near Crack Tips

Figure 1 presents a macrograph and X-ray microbeam films taken from the neighbourhood of a propagating fatigue crack tip. The diffraction arcs in film (i) reflected from the crack tip are divided into very small spots, while those in film (ii) corresponding to a place 0.40 mm from the crack tip do not contain small distinct spots. The clear formation of subgrain structure due to cyclic stress was observed only in the close vicinity of the crack tip, but not throughout the surface-depressed zone.

Dark and dispersed slip bands characteristic of slip deformation under cyclic stressing were detected near the fatigue crack tip with an optical microscope. The size of the slip band zone ahead of the crack tip ξ was found to be correlated to the gross stress amplitude σ and the crack length ℓ as

$$\xi = C_2\varsigma\,, \qquad \varsigma \equiv \left\{\sec(\pi\sigma/2C_3\sigma_Y) - 1\right\}\ell\,, \tag{1}$$

where σ_Y is the lower yield stress in monotonic tension tests, and C_2 and C_3 are empirical constants [1]. The values of C_2 and C_3 of five steels are given in Table 1. The specimens of 0.31% C steel were quenched in water and then tempered at 700°C, while those of the other steels were fully annealed at temperatures higher than the A_3-transformation temperature. The product $\sigma_{YF} \equiv C_3\sigma_Y$ indicates the yield stress

of the material in the slip band zone as described below. The value of σ_{YF} is about twice the frictional stress σ_{fr} as shown in Table 1. The slip band zone size is merely several percent of the size ζ calculated from Dugdale's equation [2]. Surface depression was observed near the fatigue crack tip under high stress intensity factors, but not under low stress intensity factors. The depressed zone size measured for the cases of high stress intensity factors was found to be smaller than that given by Dugdale's equation [3].

The distribution of the excess dislocation density D near fatigue fracture surfaces was measured by the X-ray method [1,4], and the D value was converted to the plastic strain ε by using the relation between D and plastic strain obtained in tensile deformation [5]. Figure 2 shows the results of 0.03% C steel. The plastic strain thus measured corresponds to the strain energy accumulated within the slip band zone near the crack tip. The spread η of the region with a considerable amount of plastic strain defined as given in Fig. 2 was nearly equal to about 20 percent of the slip band zone size in the case of 0.03% C steel [4].

The stress existing in a localized area of about 140 μ diameter was measured by using a new X-ray micro-camera which has a specimen-film oscillation device [4,6]. Figure 3 shows the distribution of the axial residual stress measured after the interruption of the fatigue test (open circles). The residual stress at the crack tip is compression and gradually changes to tension away from the crack tip. The values of the stress at a place 100 μ from the crack tip measured under the application of maximum tensile (an open square) and compressive loads (a solid square) are nearly equal to the fatigue yield stress of the material 30.2 kg/mm^2 and -30.2 kg/mm^2, respectively. The dot-dash line in the figure indicates the residual stress distribution calculated by using Rice's rigid plastic strip model [7] under the assumptions that the crack does not close under a tensile load and that the compression cycle of the stress does not affect the residual stress distribution. The shape of the residual stress distribution ahead of the crack tip agrees with the analytically derived curve, although the maximum compression at the crack tip is lower than the calculated value. The calculated distance from the crack tip to the point where the residual stress changes from compression to tension is twice the distance measured by the X-ray method.

Mechanisms of Fatigue Crack Propagation

The propagation rate of fatigue cracks dl/dN was correlated to each one of four microscopic parameters, i.e., the slip band zone size ahead of the crack tip ξ and the excess dislocation density D_F, the subgrain size t_F and the plastic strain ε_F on the fatigue fracture surface, where ε_F was evaluated from D_F [5]. The relation between dl/dN and ξ was found to be dependent on the specimen geometry, the loading mode and the experimental material. The material is the only factor that influences the relation dl/dN vs. D_F or t_F. On the other hand, dl/dN was expressed as a unique function of ε_F, which was not only independent of the specimen geometry and the loading mode but also of the experimental materials (0.01, 0.03 and 0.16% C steels), as shown in Fig. 4.

The micro-mechanisms of fatigue crack propagation in 0.03% C steel were comprehended in previous papers [4,8] from the observation results of microfractography and the feature of occurrence of fatigue crack growth. For the case of a propagation rate smaller than 10^{-5} mm/cycle, a fatigue crack grows intermittently along subboundaries formed ahead of the crack tip after a critical amount of excess dislocations are accumulated in subboundaries at the crack tip. The critical value of the excess dislocation density was found to equal about 2×10^{10} cm^{-2} [4]. The crack tip blunting-and-sharpening mechanism is responsible for crack growth within the rate range of $dl/dN=5\times10^{-5}\sim 2\times10^{-3}$ mm/cycle. The dl/dN versus ε_F relation given above should be explained on the basis of these micro-mechanisms.

Fatigue Crack Propagation Behavior

The results obtained in the study described in the preceding chapters will be used for the interpretation of the condition of the non-propagation of fatigue cracks and the propagation behavior of fatigue cracks under doubly repeated stress.

For a certain experimental material, the condition of the non-propagation of fatigue cracks was found to be given by a critical value of the slip band zone size ξ_c, and the ξ_c value could be calculated by substituting the critical propagation rate 4×10^{-7} mm/cycle into the dl/dN vs. ξ relation obtained at rather high propagation rates [9]. The substitution of ξ_c for ξ into Eq. (1) leads to

$$\xi_c = C_2 \zeta_c , \qquad \zeta_c = \left\{ \sec\left(\pi\sigma / 2C_3\sigma_Y\right) - 1 \right\} l , \tag{2}$$

where the value of ζ corresponding to ξ_c is denoted by ζ_c. The values of ξ_c and ζ_c for each steel are presented in Table 2. From the comparison between ζ_c and the grain size d, the ζ_c value is found to increase nearly proportionally to the size d. When σ is much smaller than σ_Y, the right hand equation given above can be rewritten as

$$K_c = 1.01\sqrt{\zeta_c\,\sigma_{YF}^2}\ , \qquad (3)$$

where K_c is the threshold stress intensity factor $K_c = 1.12\sigma\sqrt{\ell}$. The cyclic yield stress σ_{YF} was an increasing function of the frictional stress. Therefore, it can be concluded that the grain size and the frictional stress are the material parameters controlling the condition of the non-propagation of fatigue cracks.

For the case of fatigue crack propagation under doubly repeated stress, the influence of stress cycling at the first stress amplitude on the rate under the second stress amplitude was quantified with a parameter κ as

$$\kappa = K_p / K\ , \qquad (4)$$

where K is the applied stress intensity factor and K_p is the value of the stress intensity factor obtained by substituting the measured value of $d\ell/dN$ into the K vs. $d\ell/dN$ relation for constant stress amplitude fatigue. An example of the variation of κ with the increase λ of the crack length after the high-low stress level change is shown in Fig. 5, where η_v, ξ_v and ζ_v indicate the values of η, ξ and ζ just before the stress change. The minimum value of κ does not occur at $\lambda = 0$ but at $\lambda = 0.2$ mm, which means that the strain hardening due to the first stress level repetition determines the minimum rate of crack growth under the second stress level [6].

References

[1] S. Taira and K. Tanaka. Proc. Int. Conf. Mech. Behavior Mater., Kyoto, 2 (1972).
[2] D. C. Dugdale. J. Mech. Phys. Solids. 8, 100 (1960).
[3] S. Taira and K. Tanaka. To be published in J. Soci. Mater. Sci. Jap. (1973).
[4] S. Taira and K. Tanaka. To be published in Eng. Fracture Mech.
[5] S. Taira, K. Tanaka and T. Tanabe. Proc. 13th Jap. Cong. Mater. Res. 14 (1970).
[6] S. Taira, K. Tanaka and T. Shimada. To be published in J. Soci. Mater. Sci. Jap. 21 (1972).
[7] J. R. Rice. ASTM STP 415. 247 (1967).
[8] S. Taira and K. Tanaka. Proc. 15th Jap. Cong. Mater. Res. 73 (1972).
[9] S. Taira, K. Tanaka, T. Shimada and Y. Kato. To be published in Proc. 16th Jap. Cong. Mater. Res. (1973).

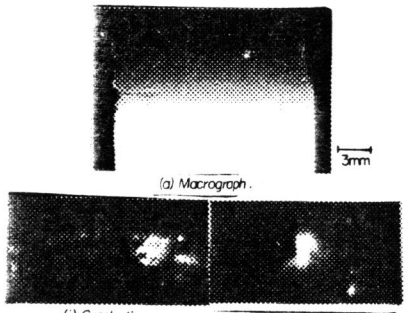

(a) Macrograph.

(i) Crack tip. (ii) 0.40mm ahead of the tip.

(b) X-ray microbeam films.

Fig.1 Observation of plastic deformation near fatigue crack tip (0.03% C steel, tension-compression, σ=13.0kg/mm^2, l=3.08 mm, K=23.3 kg/mm$^{3/2}$).

Table 1. Constants C_2 and C_3 in modified Dugdale's equation regarding slip band zone size ahead of fatigue crack tip.

Materials	σ_Y (kg/mm^2)	C_2	C_3	σ_{YF_2} (kg/mm^2)	σ_{fr} (kg/mm^2)
0.001% C iron	7.7	0.015	1.30	10.0	6.1
0.01% C steel	19.0	0.051	1.11	21.0	11.0
0.03% C steel	19.9	0.060	0.92	18.3	7.9
0.16% C steel	26.8	0.032	0.77	20.6	12.
0.31% C steel	34.7	0.086	0.87	30.2	—

$\frac{\xi}{l} = C_2\left\{\sec\left(\frac{\pi}{2}\frac{\sigma}{C_3\sigma_Y}\right)-1\right\}$, $\sigma_{YF} = C_3\sigma_Y$.

Table 2. Conditions of the non-propagation of fatigue cracks in carbon steels (Critical propagation rate is assumed to be 4×10^{-7} mm/cycle).

Materials	d (μ)	ξ_c (μ)	ζ_c (mm)	K_c (kg/mm$^{3/2}$)
0.001% C iron	450	47	3.1	17.7
0.01% C steel	50	29	0.57	16.0
0.03% C steel	40	19	0.32	10.5
0.16% C steel	24	8.0	0.27	10.8
0.31% C steel	9	11.7	0.13	11.0

$\xi_c = C_2\cdot\zeta_c$, $\zeta_c = \left\{\sec\left(\frac{\pi}{2}\frac{\sigma}{C_3\sigma_Y}\right)-1\right\}l$; $\sigma \ll \sigma_Y$, $K_c = 1.01\sqrt{\zeta_c\cdot\sigma_{YF}^2}$

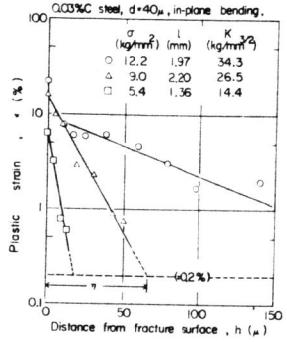

Fig.2 Distribution of plastic strain near fatigue fracture surface.

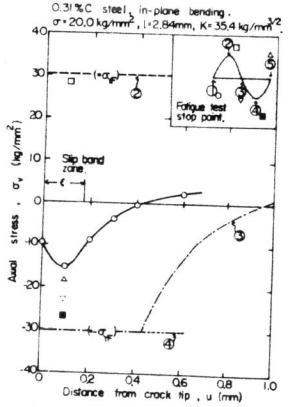

Fig.3 Axial stress distribution ahead fatigue crack tip.

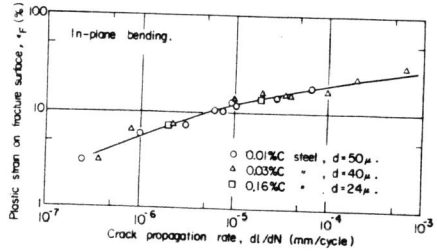

Fig.4 Relation between crack propagation rate and plastic strain on fracture surface.

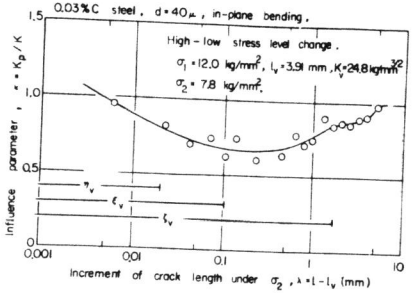

Fig.5 Crack propagation in fatigue with high-low stress level change.